Desalination and Water Treatment
www.deswater.com

doi: 10.5004/dwt.2023.29625

296 (2023) 92–100
June

Biosorption of tetracycline and Reactive blue 19 by *Pseudomonas putida* PTCC 1694 from aqueous solution

Soraya Bozorginia[a], Jalil Jaafari[a,b], Kamran Taghavi[a], Esmaeil Roohbakhsh[c], Seyed Davoud Ashrafi[a,b], Dariush Naghipour[a,*], Mehrdad Moslemzadeh[a,b,*]

[a]*Department of Environmental Health Engineering, School of Health, Guilan University of Medical Sciences, Rasht, Iran, Postcode: 4185733411, Tel.: +981333849411; Fax: +981333849413; email: dnaghipour61@gmail.com (D. Naghipour), mehrdad.moslemzadh@gmail.com (M. Moslemzadeh), sorayatrainer20@gmail.com (S. Bozorginia), jalil.jaafari@yahoo.com (J. Jaafari), kam2000ir@yahoo.com (K. Taghavi), d_ashrafi@yahoo.com (S.D. Ashrafi)*
[b]*Research Center of Health and Environment, Guilan University of Medical Sciences, Rasht, Iran*
[c]*School of Health, Guilan University of Medical Sciences, Rasht, Iran, Tel.: +981333849411; Fax: +981333849413; email: Esmaeil5115@yahoo.com (E. Roohbakhsh)*

Received 19 November 2022; Accepted 12 May 2023

ABSTRACT

In the present study, the ability of *Pseudomonas putida* biomass on biosorption of Reactive blue 19 (RB19) and tetracycline (TC) antibiotic from aqueous solutions was investigated. Both of these pollutants are harmful to human and environment safety. RB19 and TC are very resistant against the chemical process used currently in the textile industry. And also, the TC is one of the emerging antibiotics that is shown high resistant to the human-harm pathogens in the environment. These work was conducted as a batch system with variable parameters including concentration of pollutants, contact times, biomass dosages, pH, temperatures, and ionic presence. Characterization of the biosorbent was determined by scanning electron microscopy and Fourier-transform infrared spectroscopy. According to the experimental results the optimal removal efficiency obtained at pH 7, the initial concentration of pollutants 50 mg/L, the contact time 24 h, the temperature 37°C, and the sorbent dosages 0.1 g/L for TC and 1 g/L for RB19. However, the removal efficiencies for RB19 and TC increased from 62.94 to 80.25 for RB19 and from 30.69 to 54.97 for TC with increasing the biosorbent amounts. For TC, the biosorption capacity and the removal efficiency improved with increase in the TC concentration. Moreover, increasing the initial dye concentration led to enhancing biosorption capacity while the removal efficiency reduced. The highest efficiency obtained at pH 7 and 6–7 for TC and RB19, respectively. Additionally, isothermal analysis of the biosorption process agreed with the Langmuir model under (R^2 = 0.8919). The maximum biosorption capacity (q_{max}) for TC and RB19 were 19.84 and 5.94 mg/g, respectively. According to the results obtained, *P. putida* strain has a promising biosorption capacity and can be used as a native strain for bio-synergy of activated sludge in the removal of TC and RB19 compounds from aqueous solutions.

Keywords: Pseudomonas putida; Tetracycline antibiotic; Reactive blue dye; Biosorption

1. Introduction

Most of the emerging pollutants passes through the conventional wastewater treatment processes and enters to the environment. Therefore, finding a promising process to remove these pollutants is very needed [1,2]. Due to the widespread use of primary compounds causing the emerging pollutants in the modern human life, these pollutants

* Corresponding authors.

are constantly entering the environment from countless sources [3]. One of the most important ways of production of these pollutants in the industrial processes can be attributed to the activities of the pharmaceutical industry (due to the biggest main concern of drug contamination, that is, the group of antibiotics in terms of production and consumption worldwide) and textile industries (because of chemical dye's consumption in a range of near ten thousand different types) [4,5].

Dyes are the largest groups of organic compounds, lead to the formation of colored wastewaters. Meanwhile, reactive dyes are water-soluble anionic dyes. These dyes have largely replaced the direct and azo dyes [6]. Reactive dyes are mainly used for dyeing cellulose fibers such as cotton and viscose. The reactive dyes are available in a wide range and they are used with a large number of dyeing techniques. In dyeing cellulose fibers with reactive dyes, the following chemicals and auxiliaries are used [7]:

- Alkali (sodium carbonate, bicarbonate and caustic soda);
- Salt (mainly sodium chloride and sulphate);
- Urea may be added to the padding liquor in continuous processes;
- Sodium silicate may be added in the cold pad-batch method.

However, they are widely used in the textile industry due to their ease of use and low energy consumption [8]. Reactive blue 19 (RB19) is one of these dyes which is an anthraquinone dye in terms of color factor and resistance to the chemical processes that is currently used in the textile industry [9]. RB19 dye structure are shown in Fig. 1.

The presence of antibiotic-resistant bacteria in aquatic environments is the most important concern associated with emerging pathogens in the environment [10]. Researches showed that antibiotics are poorly absorbed in the body organs, so most of these substances or their metabolites do not change or enter sewer systems. The lipophilic property of antibiotics cause to their stability and therefore they can remain in the environment for a long time. However, their presence in the human body even low concentrations is dangerous for the organs [11,12].

Pseudomonas putida bacterium has shown a high resistant against these antibiotics in a variety of environments. According to the literatures, *P. putida* is well able to degradation of antibiotics. The production of biosurfactants by *P. putida,* via increasing the emulsification of cyclic compounds and alter surface tension and binding to the bacterial cell surface, is responsible for that ability [8,13]. Generally, the mechanisms involved in the biosorption process include forming complexes, biological adsorption, ion exchange, chelating micro precipitation, and oxidation and reduction reactions [14,15].

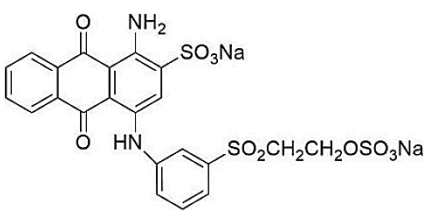

Fig. 1. Structure of Reactive blue 19 dye.

Objective of the present study was to use of the *P. putida* bacterium as a biosorbent in removing RB19 dye and antibiotics. For this purpose, the performance of biosorbent has been determined by examining the parameters including contact time, pH, dye's and antibiotic's concentrations, biosorbent dosage, and ionic presence effects. Moreover, isotherm studies were also studied [16].

2. Material and methods

2.1. Reagents

RB19 and tetracycline antibiotic powder (>99%) were from Alvan Sabet Company, Iran and Sigma-Aldrich, USA, respectively. *P. putida* strain (DSM 291) PTCC1694 was supplied by Collections and Industrial Bacteria Institute, Iran. *P. putida* is a gram-negative bacterium, rod-shaped, and belongs to the group of soil saprotrophic bacteria. This strain was in aerobic conditions at 37°C and pH = 7 in the environment containing; beef extract, pepton, and agar. After culturing on nitrite agar as a storage medium, *P. putida* was maintained with periodic culturing at 4°C on plates containing nitrite agar to conduct the experiments. In all the steps of experiment, parameters such as temperature and speed of the shaker were fixed at 37°C and 104 rpm, respectively. In order to perform the experiments, 250 mL Erlenmeyer flasks were used as batch reactors.

2.2. Tetracycline and RB19 biosorption experiments

In the present study the biosorption experiments were designed based on one factor at the time. The studied parameters and range for removal of tetracycline were as follow: biomass concentration (0.3, 0.1, 0.5, and 1 g/L), tetracycline concentration (5, 10, 20, 50, and 100 mg/L), temperature (25°C, 35°C, and 42°C), and contact time (6, 12, 24, 48, and 72). To study the Reactive blue 19 dye biosorption, the studied parameters were including biomass concentration (0.3, 0.1, 0.5, and 1 g/L), dye concentration (5, 10, 20, 50, and 100 mg/L), temperature (25°C, 35°C, and 42°C), and contact time (6, 12, 24, 48, and 72). In overall the biosorption processes, pH of the experimental solutions were adjusted to 7 with 0.1 mL of hydrochloric acid and 0.1 mL soda. In order to investigate the equilibrium isotherm, an experiment was conducted on the optimal biomass dosage and with concentration of 250 cc for both pollutants at the optimal pH. The resulting mixture was stirred at 37°C in an incubator shaker (104 rpm) for 24 h.

2.3. Analytical measurements

Residuals of tetracycline and RB19 dye concentrations were determined using the UV-Visible spectrophotometric method, as standard methods for the examination of water and wastewater [17]. The samples were measured in the wavelengths of 348 and 591 nm for tetracycline and RB19 dye, respectively, with DR5000 UV/Vis, HACH. And also, bacterial density of the samples containing biomass, after filtering, was determined with the mentioned spectrophotometer at the corresponding wavelength. However, the

standard calibration curves were drawn with measuring the different concentrations of tetracycline and RB19 dye in the wavelengths of 348 and 591 nm, respectively, and the final concentration of these compounds was extracted from the calibration curve after the biosorption process. The concentrations of pollutants were 0.1, 0.5, 1, 2, 3, 4, 5, 6, 7, 8, 9, and 10 mg/L. The pH of aqueous solutions was measured with a digital electronic pH meter system.

3. Result and discussion

3.1. Biomass characterization

In order to determine the size and shape of the biomass after drying and turning into powder, the scanning electron microscopy (SEM) was used.

Fourier-transform infrared spectroscopy (FTIR) is a new method to detect bacteria [18]. FTIR is based on the absorption of radiation and the study of vibration jumps in multi-atomic molecules and ions. This method is mainly used to identify organic compounds, because the spectra of these compounds are generally complex and have a large number of maximum and minimum peaks that can be used for comparative purposes. Each bacterium has a cell wall/membrane complex that combines its own fingerprint spectrum due to the stretching and vibration of the bonding molecule in the functional groups in proteins, nucleic acids, lipids, sugars, and lipopolysaccharides. Molecules is different in each species. That's why each bacterium has its own range. However, SEM and FTIR analyzes were used to evaluate the shape and structure and *P. putida* biomass. Fig. 2a and b show a microscopic image of the microbial biomass of *P. putida* before and after adsorption, respectively. FTIR spectra are shown in Fig. 3. The range of this spectra was from 500–4,000 cm^{-1}. A wide range of strong peak at wavelengths of 3,407 cm^{-1} is associated with –NH and –OH stretching vibration bands of alcoholic and amide functional group. The peak at 2,928 cm^{-1} corresponded to the –CH stretching vibration of $–CH_3$ and $–CH_2$ group [19]. The peak at 1,633 cm^{-1} is related to the stretching band of the amide I and II group. The peak at 1,404 cm^{-1} is related to C=O symmetric stretching of carboxyl salt (–COOH). The peak at 1,112 cm^{-1} can correspond to vibration of carboxyl (–COOH) and phosphate groups (P=O and P–O) of the tripolyphosphate [20]. A strong peak at 1,066 cm^{-1} can be attributed to C–O stretching of alcohols and carboxylic acids. The peaks related to the fingerprint region (543 and 619 cm^{-1}) is ascribed to weak absorption bands but it is unique. In general, the IR spectra are indicative of this fact that main functional groups on the biomass surface include hydroxyl,

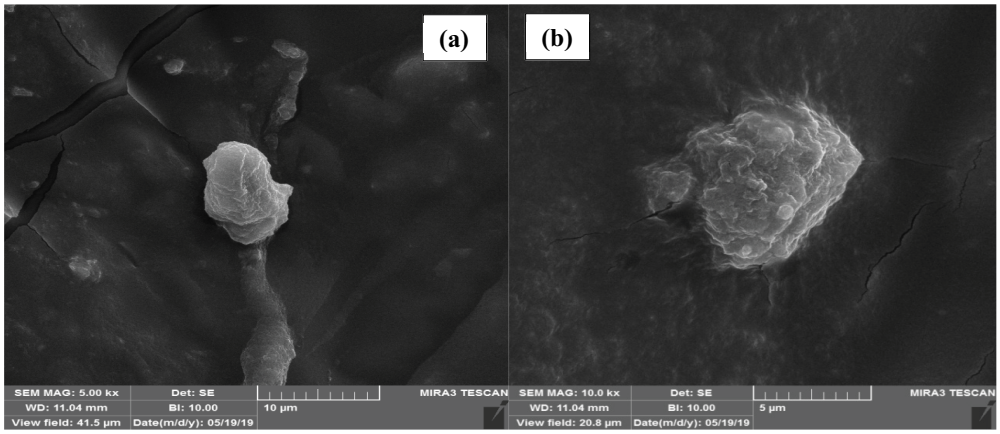

Fig. 2. Scanning electron microscopy image of native *Pseudomonas putida* before (a) and after (b) adsorption.

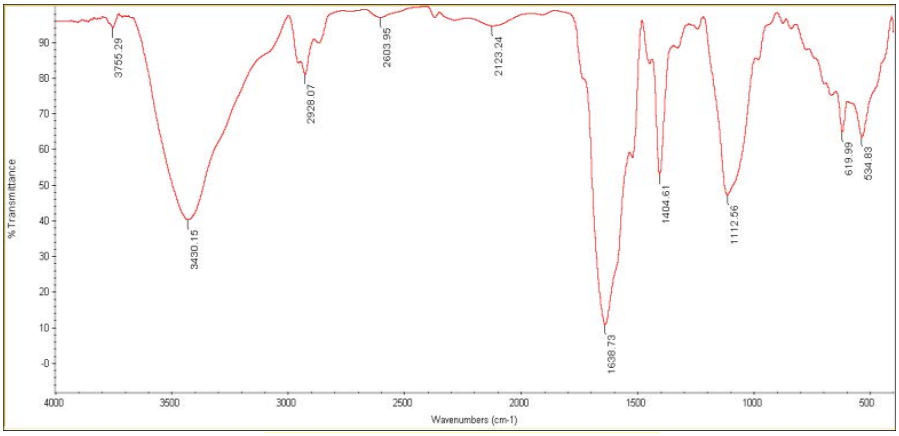

Fig. 3. Fourier-transform infrared spectra of *Pseudomonas putida* biomass.

carboxyl, sulphonate, amide, imidazole, phosphate and phosphodiester groups.

3.2. Effect of the adsorbent dosage

The effect of *P. putida* biosorbent dosage on removal tetracycline (TC) and RB19 biosorption is shown in Fig. 4. This analysis was conducted using the biosorbent dosage from 0.64 to 6.4 g/L for tetracycline and from 2.6 to 11.3 g/L RB19 for RB19 dye. The results indicate that an increase in biosorbent dosage from 0.64 to 6.4 g/L lead to decreasing the biosorption capacity from 23.78 to 4.26 mg/g for tetracycline while increasing the biosorbent dosage from 2.6 to 11.3 g/L reduced the biosorption capacity from 12.06 to 3.21 mg/g. The results show that in low biomass dosage, the biosorption capacity is higher than that in high biomass dosage. These results are attributed to the availability of active unsaturated sites for organic bonds. That means which at constant pollution concentrations, in lower biosorbent dosages all of the sorbents capacities were fully occupied, while in the higher dosages, the capacities were not fully occupied [21,22]. Another hand, the removal efficiencies for RB19 and TC were developed from 62.94 to 80.25 for RB19 and from 30.69 to 54.97 for TC by increasing the biosorbent value. This difference in efficiencies for RB19 and TC is related to the strong attraction strength of RB19 with the biosorbent surface.

3.3. Effect of initial concentration of TC and Reactive blue 19 on the sorption process

Effect of the initial concentration of dye on the removal efficiency was carried out by varying the initial concentration of pollutants, that is, tetracycline (1, 5, 10, 20, and 50 mg/L), and RB19 (20, 30, 40 and 50 mg/L). The other experimental conditions were optimal pH (7), and biosorbent dosage (1 g/L for RB19 dye and 0.1 g/L for tetracycline). The obtained results are depicted in Fig. 5. As can be seen, the biosorption capacity increased with increasing the initial concentration of pollutants. When the initial concentration of TC increased from 1 to 50 mg/L, the capacity increased from 0.21 to 35.77 mg/g. Moreover, increasing initial dye concentration 20 to 50 mg/L has led to enhancing biosorption capacity from 2.13 to 4.65 mg/g. Additionally, the results were indicative of this fact that reducing the initial concentration of TC will be associated with the development of the removal efficiency. The reason for this phenomenon is the equality of the free hydroxyl radical ($OH^{\bullet}$) with the number of the biosorption sites on the biosorbent surface [1]. Therefore, the samples with lower TC concentrations with the same hydroxyl radical will have more chance for degradation compared to the samples with a higher concentration of antibiotics. In the lower initial concentrations of reactants, the ratio of the initial number of sorbate molecules to the active biosorption sites are low, and as a result, the biosorption will independent of the initial concentration [16].

3.4. Effect of pH and ionic strength on the adsorption of TC and RB19

One of the most important factors influencing the biosorption capacity is the pH of the solution. The biosorption efficiency depends on the pH of the solution because changes in pH lead to changes in the degree of ionization of the biosorbent molecule and the properties of the biosorbent

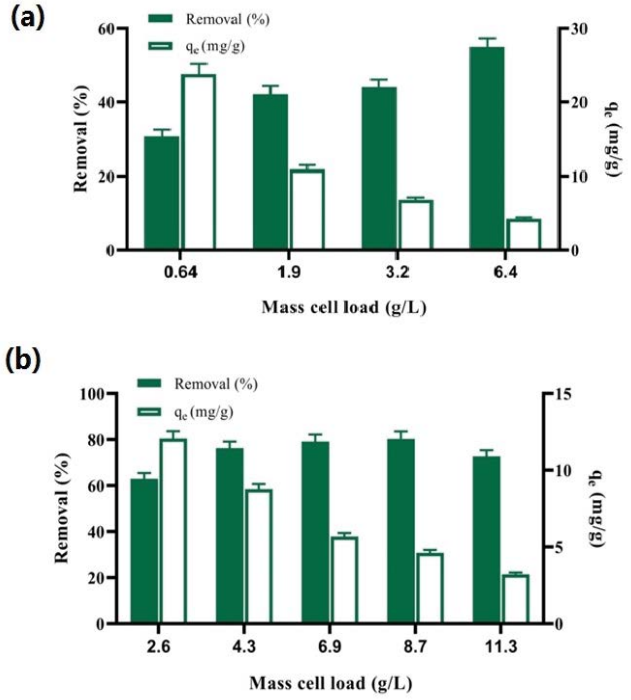

Fig. 4. Percentage removal of (a) tetracycline and (b) Reactive blue 19 by *Pseudomonas putida* within 24 h.

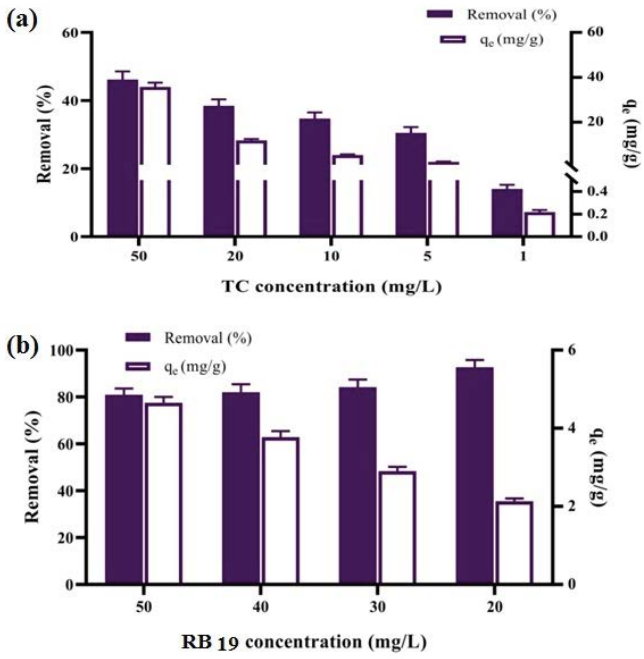

Fig. 5. Effect of initial tetracycline concentration on percentage adsorption: the percentage removal of (a) tetracycline and (b) Reactive blue 19 by *Pseudomonas putida* within 24 h.

surface. The effect of solution pH on the rate of removal of TC and RB19 by *P. putida* strain was investigated in the range of 5–9. The results show that the highest amount of biosorption was performed at pH = 7. It is clear that the pH changes affect the TC biosorption (Fig. 6), because the pH affects both the biosorbent charge and the TC charge. In this pH range, the maximum biosorption rate was obtained at pH = 7, and in contrast, in the pH values less and more than this, biosorption capacity decreased.

Due to the weak acid separation of the TC molecule, it can be seen that electrostatic attraction and the formation of ionic bonds were not the main mechanisms in the biosorption process [23]. The interaction of π–π bonds in the benzene rings of the TC molecule with the biosorbent surface is one of the most important biosorption parameters. Now, regarding the RB19 dye, it is an anionic dye with positive charge due to having the negative groups of sulfonates in its molecular structure; therefore, the dye biosorption is desirable due to the positive charge on it ($pH > pH_{PZC}$) [24].

3.5. Effect of reaction time on the biosorption of TC

Biosorption capacity and efficacy of TC and color removal by *P. putida* biomass are prepared as Fig. 7. The results showed that the removal efficiency increases with increasing contact time. However, the highest biosorption rate is obtained for TC in the first 6 h and for dye in the first 12 h. Then, the biosorption rate had a mild trend until it reaches equilibrium. The dye biosorption capacity reached equilibrium after 12 h of reaction time. After this, the biosorption capacity of biomass and dye removal efficiency has not changed anymore. In this equilibrium, the biosorption capacity and dye removal efficiency were 3.99 mg/g and 69.59%, respectively.

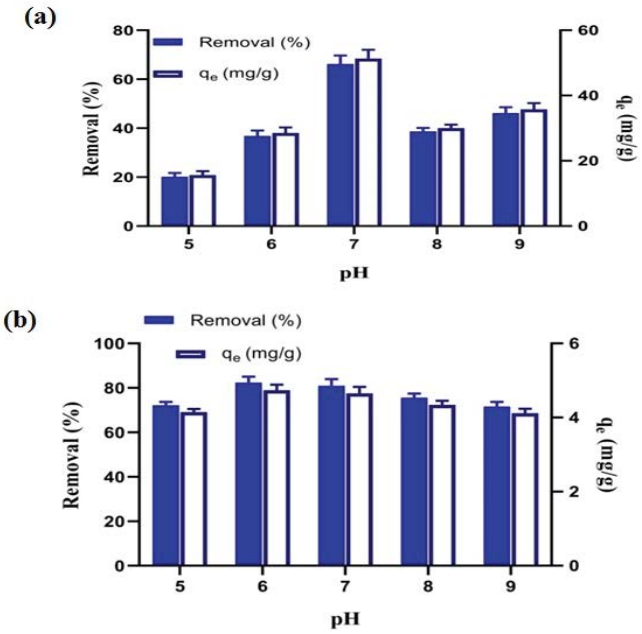

Fig. 6. Effect of pH on percentage adsorption: the percentage removal of (a) tetracycline and (b) Reactive blue 19 by *Pseudomonas putida* within 24 h.

It is clear that biosorption by *Pseudomonas* biomass has occurred in two phases. The greater biosorption in the initial phase is related to the more vacant sites at the beginning of the process. In the next phase, the problem is that the remaining vacant sites are not occupied due to the repulsive force of the dye ions in the liquid phase [25]. Subsequent microbial precipitation and saturation of the connection sites in the next phase involve slower ionic interaction [26]. The results of this study were consistent with the studies conducted for the removal of azo dyes by *Rhizopus arrhizus* and lead removal by *Lysinibacillus fusiformis*, the initial contact time of these studies were 15–20 min and 60 min, respectively [6,13].

3.6. Effect of temperature on the biosorption of TC

Temperature is another important parameter in the study of biosorption processes. Fig. 8 is depicted the results of the temperature effects on the biosorption process of TC and RB19 dye by *P. putida*. The range of selected temperatures were to be 25°C, 35°C, and 45°C. Increasing the temperature damages the attraction forces between active sites and TC molecules, and more variable complex shape is made, and the rate of biosorption capacity increases. The study conducted by Parajuli and Hirota [27] is in agreement with the results of the present study.

3.7. Effect of influence of ions on the process of adsorption

Pharmaceutical and textile industry wastewaters contain a variety of suspended solids and soluble compounds

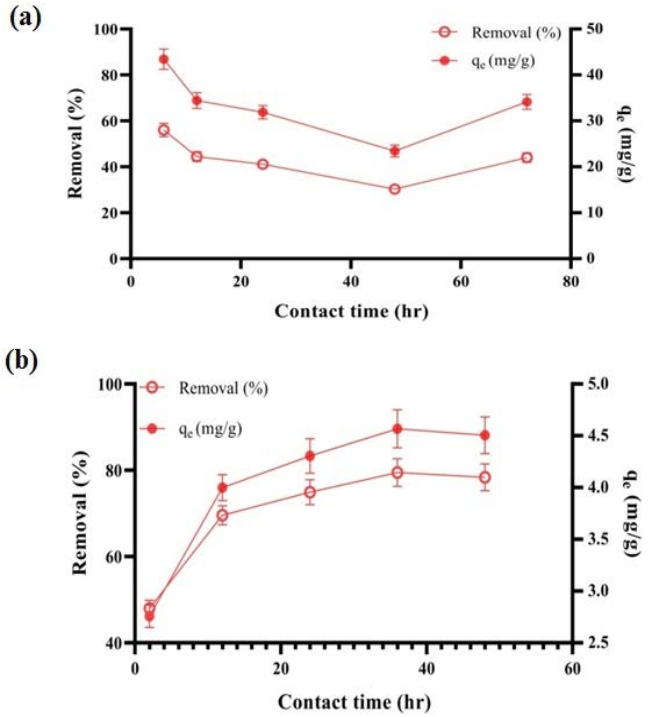

Fig. 7. Effect of contact time on percentage adsorption: the percentage removal of (a) tetracycline and (b) Reactive blue 19 by *Pseudomonas putida* within 24 h.

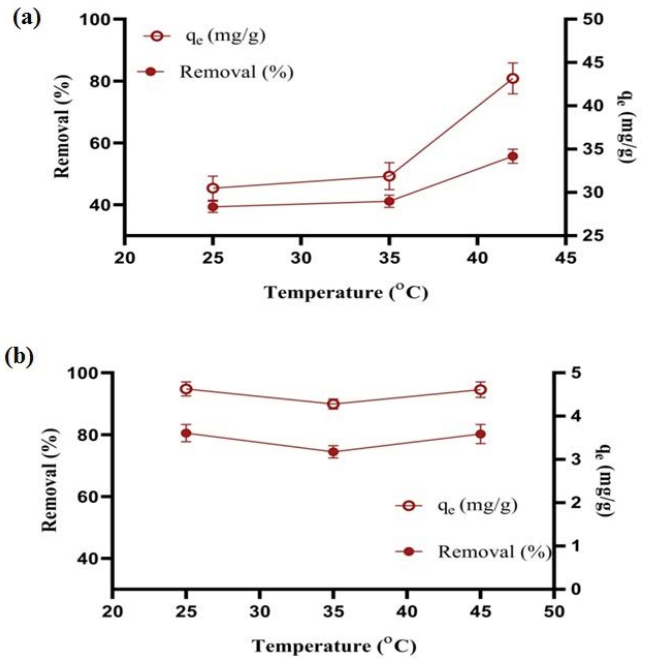

Fig. 8. Effect of temperature on percentage adsorption: the percentage removal of (a) tetracycline and (b) Reactive blue 19 by *Pseudomonas putida* within 24 h.

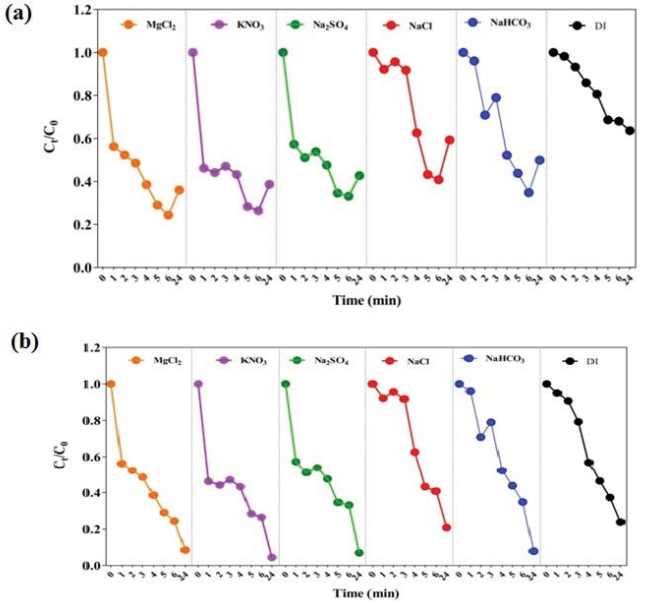

Fig. 9. Effect of ions on the biosorption of tetracycline (a) and Reactive blue 19 (b).

that are considered as impurities in the removal process. These impurities include cations (Na^+, NH^{4+}, Ca^{2+}) and ions (Cl^-, NO_3^-, CO_3^-), which are most of the metal ions present in wastewater in the pharmaceutical and textile industries [2]. Fig. 9 shows the effect of ions on the biosorption of TC and Reactive blue 19. The results show that with increasing ions, the biosorption potential increased. The ions effect on dye biosorption is higher than that of TC. The presence of sulfonic functional group (R-SO_3Na) on chromophore of RB19 dye causes a positive charge, and the presence of ions increases the electrical charge of the cell surface [28]. The presence of chloride and bicarbonate salts has resulted in a very positive charge on the cellular sorbent surface, which greatly reduces the electrostatic repulsive force [29]. Thus, the promoting order on TC and RB19 biosorption by inorganic ions followed the sequence $HCO_3^- > Cl^- \approx\rightarrow NO_3^- \approx SO_4^{+2} > Na^+, K^+$ for TC and $NO_3^- \approx SO_4^{+2} \approx K^+ \approx HCO_3^- \approx Cl^- > Na^+, K^+$ for RB19.

3.8. Equilibrium studies

In this study, the biosorption behavior of Reactive blue 19 dye and TC was tested by Freundlich (1) and Langmuir isotherms to determine the best adsorption state for this type of adsorbent. Langmuir adsorption isotherm is more useful for single-layer adsorbents. In this type of isotherm, a layer of dissolved substance molecules is absorbed onto adsorbent, and at all adsorbent surfaces, the amount of adsorbed energy is assumed to be the same and adsorption bonds are presumed reversible [22,30].

3.8.1. Langmuir isotherm

$$q_e = \frac{q_m k_l c_e}{1 + k_l c_e} \tag{1}$$

where q_e: amount of substance adsorbed per unit mass of adsorbent (mg/g); C_e: concentration of the adsorbate in the liquid phase before reaching the equilibrium state (mg/g); q_{max}: maximum adsorption capacity (mg/kg); k_l: Langmuir isotherm constant, which is determined for each system at a given temperature (mg/L).

3.8.2. Freundlich isotherm

$$\log q_e = \log k_F + \frac{1}{n} \log C_e \tag{2}$$

where q_e: amount of substance adsorbed per unit mass of adsorbent (mg/g); C_e: concentration of the adsorbate in the liquid phase before reaching the equilibrium state (mg/g); k_F, n: Freundlich isotherm constants are related to the capacity and energy of adsorption.

Given that one of the assumptions of the Freundlich isotherm model is that the process of adsorption occurs at the heterogeneous (multi-layered) energy levels, this model indicates that the surface of adsorbent used is not uniform.

The Langmuir characteristics parameters and the correlation coefficient with respect to this equation are given in Table 1. And the resulting plots are shown in Fig. 10.

Examination of adsorption equilibrium and mechanisms affecting it shows that the biosorption process of TC and RB19 dye follows the Langmuir isotherm. This conclusion is based on the correlation coefficient of the equation of each isotherm. Isotherm constants are shown in Table 1. The results show that the biosorption of RB19 on the biomass,

Table 1
Values of the Langmuir and Freundlich adsorption isotherm for tetracycline and Reactive blue 19

Contaminant	Biosorbent	Langmuir isotherm			Freundlich isotherm		
		q_{max} (mg/g)	b (L/mg)	R^2	k_F (mg/g)	n	R^2
Tetracycline	Living	19.84	0.032	0.428	0.207	0.681	0.994
Reactive blue 19 dye	Living	5.94	0.278	0.898	3.64	2.52	0.936

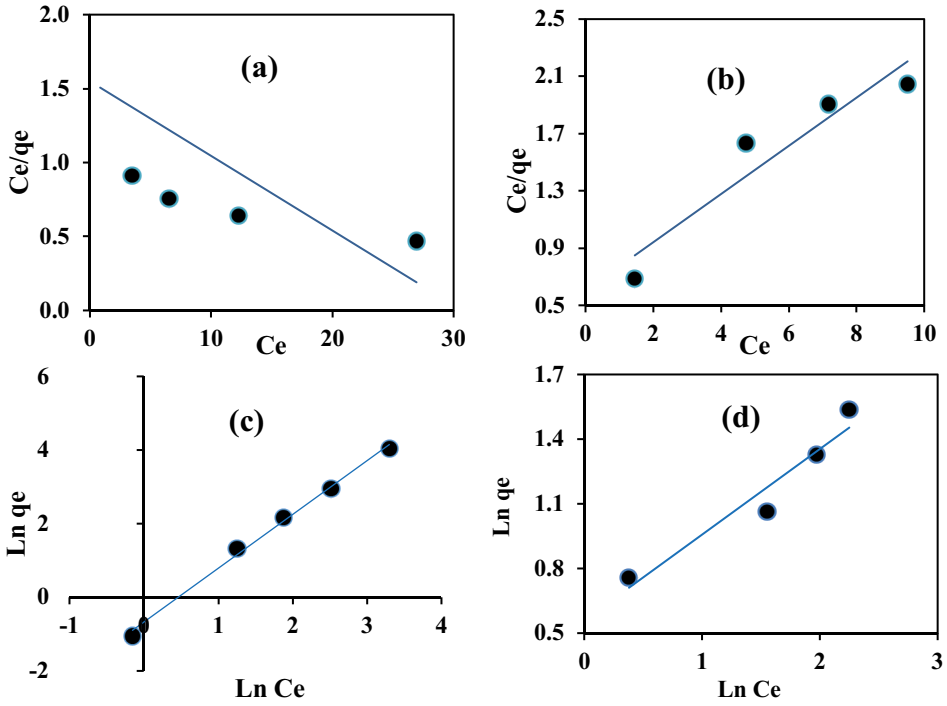

Fig. 10. Langmuir and Freundlich isotherms for the biosorption of tetracycline (a and c) and Reactive blue 19 (b and d) by *Pseudomonas putida* bacteria.

Table 2
Comparison of biosorption capacity of studied biosorbent with other biosorbents

Compound	Biosorbent	q (mg/g)	Experimental conditions	References
Pb(II)	*Pseudomonas aeruginosa*	53.9	pH = 6.2, 29°C	[32]
Pb(II)	*Lysinibacillus fusiformis*	54.64	pH = 6.2, 27°C	[33]
Pb(II)	*Bacillus badi*us	1.65	pH = 4.5, 30°C	[34]
Acid red 88	*Ulva reticula*ta	16.54	pH = 7	[35]
Trypan blue	*Aeromonas hydrophila* RC1	13.091	pH = 7, 28°C	[36]
Tetracycline	*Pseudomonas putida*	19.84	pH = 7, 35°C	This work
Reactive blue 19	*Pseudomonas putida*	5.94	pH = 7, 35°C	This work

according to the correlation coefficient of 0.89, follows the Langmuir isotherm, and the maximum biosorption capacity based on Langmuir model was 5.94 mg/g biosorbent. The biosorption of TC on biomass follows the Langmuir isotherm coefficient with respect to the correlation coefficient of 0.42, and the maximum biosorption capacity of the Langmuir model was 19.84 mg/g of biosorption [31].

3.9. Comparison of adsorption capacity with the biosorbent

The biosorption capacity of TC and Reactive blue 19 on studied biosorbent was compared with other biosorbents in Table 2. Different biosorption capacities depend on the biosorbent characteristics and chemical structure of the reactants [6].

4. Conclusion

In this study, the *P. putida* bacterium was used for biosorption of TC and RB19 dye. As obtained results, below cases are concluded.

- Removal rate of TC is more sensitive than that for RB19 dye on increasing the biosorbent mass.
- *P. putida* biosorbent could be more applicable for treatment real water because of its well efficiency at natural pH, 6–7.
- Water in high temperatures would be well target to *P. putida* biosorbent for removal of TC. That is while RB19 dye was well removed in a broad range of temperatures.
- In further studies, it will be hope to improve the removal efficiency and time reduction by adding some functional groups. And also, it will be good to apply that on real water and wastewater.
- Finally, the biosorbent derived from *P. putida* would be a promising sorbent to remove of TC and RB19 dye from aqueous solutions. The effect of the parameters studied on the process was significant.

Acknowledgement

This article is taken from the Master's thesis of Environmental Health Engineering, Guilan University of Medical Sciences with ethics code IR.GUMS.REC.1399.599 and grant number 99080503. The authors thank and appreciate deputy of research and technology of university for their financial support and the expert of the water and sewage laboratory of the faculty of health who helped in the implementation of this research.

References

[1] D. Naghipour, L. Hoseinzadeh, K. Taghavi, J. Jaafari, Characterization, kinetic, thermodynamic and isotherm data for diclofenac removal from aqueous solution by activated carbon derived from pine tree, Data Brief, 18 (2018) 1082–1087.
[2] M. Seyedsalehi, J. Jaafari, C. Hélix-Nielsen, G. Hodaifa, M. Manshouri, S. Ghadimi, H. Hafizi, H. Barzanouni, Evaluation of moving-bed biofilm sequencing batch reactor (MBSBR) in operating A^2O process with emphasis on biological removal of nutrients existing in wastewater, Int. J. Environ. Sci. Technol., 15 (2018) 199–206.
[3] E. Demirbas, M.Z. Nas, Batch kinetic and equilibrium studies of adsorption of Reactive Blue 21 by fly ash and sepiolite, Desalination, 243 (2009) 8–21.
[4] J. Jaafari, A.B. Javid, H. Barzanouni, A. Younesi, N.A.A. Farahani, M. Mosazadeh, P. Soleimani, Performance of modified one-stage phoredox reactor with hydraulic up-flow in biological removal of phosphorus from municipal wastewater, Desal. Water Treat., 171 (2019) 216–222.
[5] J. Jaafari, K. Yaghmaeian, Response surface methodological approach for optimizing heavy metal biosorption by the blue-green alga chroococcus disperses, Desal. Water Treat., 142 (2019) 225–234.
[6] N.A. Salvi, S. Chattopadhyay, Biosorption of azo dyes by spent *Rhizopus arrhizus* biomass, Appl. Water Sci., 7 (2017) 3041–3054.
[7] B.A. Marinho, R.O. Cristóvão, R. Djellabi, J.M. Loureiro, R.A.R. Boaventura, V.J.P. Vilar, Photocatalytic reduction of Cr(VI) over TiO_2-coated cellulose acetate monolithic structures using solar light, Appl. Catal., B, 203 (2017) 18–30.
[8] J.P. Bound, N. Voulvoulis, Predicted and measured concentrations for selected pharmaceuticals in UK rivers: implications for risk assessment, Water Res., 40 (2006) 2885–2892.
[9] D. Naghipour, K. Taghavi, J. Jaafari, Y. Mahdavi, M. Ghanbari Ghozikali, R. Ameri, A. Jamshidi, A. Hossein Mahvi, Statistical modeling and optimization of the phosphorus biosorption by modified *Lemna minor* from aqueous solution using response surface methodology (RSM), Desal. Water Treat., 57 (2016) 19431–19442.
[10] A. Dehghan, A. Zarei, J. Jaafari, M. Shams, A. Mousavi Khaneghah, Tetracycline removal from aqueous solutions using zeolitic imidazolate frameworks with different morphologies: a mathematical modeling, Chemosphere, 217 (2019) 250–260.
[11] D. Naghipour, A. Amouei, K. Taher Ghasemi, K. Taghavi, Removal of metoprolol from aqueous solutions by the activated carbon prepared from pine cones, Environ. Health Eng. Manage., 6 (2019) 81–88.
[12] S. Nethaji, A. Sivasamy, A.B. Mandal, Adsorption isotherms, kinetics and mechanism for the adsorption of cationic and anionic dyes onto carbonaceous particles prepared from *Juglans regia* shell biomass, Int. J. Environ. Sci. Technol., 10 (2013) 231–242.
[13] K. Mathivanan, R. Rajaram, G. Annadurai, Biosorption potential of *Lysinibacillus fusiformis* KMNTT-10 biomass in removing lead(II) from aqueous solutions, Sep. Sci. Technol., 53 (2018) 1991–2003.
[14] M.J. Puchana-Rosero, E.C. Lima, S. Ortiz-Monsalve, B. Mella, D. da Costa, E. Poll, M. Gutterres, Fungal biomass as biosorbent for the removal of Acid Blue 161 dye in aqueous solution, Environ. Sci. Pollut. Res., 24 (2017) 4200–4209.
[15] A. Ramesh, H. Hasegawa, W. Sugimoto, T. Maki, K. Ueda, Adsorption of gold(III), platinum(IV) and palladium(II) onto glycine modified crosslinked chitosan resin, Bioresour. Technol., 99 (2008) 3801–3809.
[16] M. Karimpour, S.D. Ashrafi, K. Taghavi, A. Mojtahedi, E. Roohbakhsh, D. Naghipour, Adsorption of cadmium and lead onto live and dead cell mass of *Pseudomonas aeruginosa*: a dataset, Data Brief, 18 (2018) 1185–1192.
[17] D. Naghipour, K. Taghavi, M. Moslemzadeh, Removal of methylene blue from aqueous solution by Artist's Bracket fungi: kinetic and equilibrium studies, Water Sci. Technol., 73 (2016) 2832–2840.
[18] N. El Messaoudi, M. El Khomri, E.-H. Ablouh, A. Bouich, A. Lacherai, A. Jada, E.C. Lima, F. Sher, Biosynthesis of SiO_2 nanoparticles using extract of *Nerium oleander* leaves for the removal of tetracycline antibiotic, Chemosphere, 287 (2022) 132453, doi: 10.1016/j.chemosphere.2021.132453.
[19] N. El Messaoudi, M. El Khomri, A. Dabagh, Z.G. Chegini, A. Dbik, S. Bentahar, A. Lacherai, M. Iqbal, A. Jada, F. Sher, É.C. Lima, Synthesis of a novel nanocomposite based on date stones/$CuFe_2O_4$ nanoparticles for eliminating cationic and anionic dyes from aqueous solution, Int. J. Environ. Stud., 79 (2022) 417–435.
[20] Mu. Naushad, Surfactant assisted nano-composite cation exchanger: development, characterization and applications for the removal of toxic Pb^{2+} from aqueous medium, Chem. Eng. J., 235 (2014) 100–108.
[21] A. Jonidi, M. Moslemzadeh, Adsorption of lead (Pb^{2+}) onto salicylic acid-methanol modified steel slag from aqueous solution: a cost analysis, Desal. Water Treat., 198 (2020) 200–210.
[22] S. Pourkarim, F. Ostovar, M. Mahdavianpour, M. Moslemzadeh, Adsorption of chromium(VI) from aqueous solution by Artist's Bracket fungi, Sep. Sci. Technol., 52 (2017) 1733–1741.
[23] Y. Wang, F. Wang, Y. Feng, Z. Xie, Q. Zhang, X. Jin, H. Liu, Y. Liu, W. Lv, G. Liu, Facile synthesis of carbon quantum dots loaded with mesoporous g-C_3N_4 for synergistic absorption and visible light photodegradation of fluoroquinolone antibiotics, Dalton Trans., 47 (2018) 1284–1293.
[24] R. Zandipak, S. Sobhanardakani, Novel mesoporous Fe_3O_4/SiO_2/CTAB-SiO_2 as an effective adsorbent for the removal of amoxicillin and tetracycline from water, Clean Technol. Environ. Policy, 20 (2018) 871–885.

[25] H. Wang, S. Shen, L. Liu, Y. Ji, F. Wang, Effective adsorption of phosphate from wastewaters by big composite pellets made of reduced steel slag and iron ore concentrate, Environ. Technol., 36 (2015) 2835–2846.
[26] Y. Huang, J. Guo, P. Yan, H. Gong, F. Fang, Sorption–desorption behavior of sulfamethoxazole, carbamazepine, bisphenol A and 17A-ethinylestradiol in sewage sludge, J. Hazard. Mater., 368 (2019) 739–745.
[27] D. Parajuli, K. Hirota, Recovery of palladium using chemically modified cedar wood powder, J. Colloid Interface Sci., 338 (2009) 371–375.
[28] M.A.N. Khan, M. Siddique, F. Wahid, R. Khan, Removal of Reactive blue 19 dye by sono, photo and sonophotocatalytic oxidation using visible light, Ultrason. Sonochem., 26 (2015) 370–377.
[29] N.S. Maurya, A.K. Mittal, P. Cornel, E. Rother, Biosorption of dyes using dead macro fungi: effect of dye structure, ionic strength and pH, Bioresour. Technol., 97 (2006) 512–521.
[30] D.Q. Melo, V.O.S. Neto, J.T. Oliveira, A.L. Barros, E.C.C. Gomes, G.S.C. Raulino, E. Longuinotti, R.F. Nascimento, Adsorption equilibria of Cu^{2+}, Zn^{2+}, and Cd^{2+} on EDTA-functionalized silica spheres, J. Chem. Eng. Data, 58 (2013) 798–806.
[31] I. Vishan, S. Sivaprakasam, A. Kalamdhad, Isolation and identification of bacteria from rotary drum compost of water hyacinth, Int. J. Recyl. Org. Waste Agric., 6 (2017) 245–253.
[32] S. Vimalnath, H. Ravishankar, C. Schwandt, R.V. Kumar, S. Subramanian, Mechanistic studies on the biosorption of Pb(II) by *Pseudomonas aeruginosa*, Water Sci. Technol., 78 (2018) 290–300.
[33] R. Sharma, T. Jasrotia, A. Umar, M. Sharma, S. Sharma, R. Kumar, A.A.M. Alkhanjaf, R. Vats, V. Beniwal, R. Kumar, J. Singh, Effective removal of Pb(II) and Ni(II) ions by *Bacillus cereus* and *Bacillus pumilus*: an experimental and mechanistic approach, Environ. Res., 212 (2022) 113337, doi: 10.1016/j.envres.2022.113337.
[34] R. Gallegos-Monterrosa, S. Kankel, S. Götze, R. Barnett, P. Stallforth, Á.T. Kovács, *Lysinibacillus fusiformis* M5 induces increased complexity in *Bacillus subtilis* 168 colony biofilms via hypoxanthine, J. Bacteriol., 199 (2017), doi: 10.1128/jb.00204-17.
[35] A. Saravanan, Equilibrium and kinetic modeling of Acid red 88 (AR 88) biosorption by *Ulva reticulata*, Int. J. Chem. Process Eng. Res., 1 (2014) 19–31.
[36] S. Busi, R. Chatterjee, J. Rajkumari, S. Hnamte, Ecofriendly biosorption of dyes and metals by bacterial biomass of *Aeromonas hydrophila* RC1, J. Environ. Biol., 37 (2016) 267–274.